

X-ray Diffraction Study on the Structure of Concentrated Aqueous Solutions Involving Alanine Molecules with Different Optical Activities

Yasuo Kameda,*[1] Aya Okuyama,[1] Yuko Amo,[1] Takeshi Usuki,[1] and Shinji Kohara[2]

[1]Department of Material and Biological Chemistry, Faculty of Science, Yamagata University, Yamagata 990-8560

[2]Japan Synchrotron Radiation Research Institute, Sayo, Hyogo 679-5198

Received May 28, 2007; E-mail: kameda@sci.kj.yamagata-u.ac.jp

X-ray diffraction measurements on aqueous 2.5 mol % DL-, L-, and D-alanine solutions in D_2O were carried out at 26 ± 2 °C in order to obtain information concerning the difference in the hydrogen-bonded structure between aqueous solutions involving amino acid molecules with different optical activities. The difference function, $\Delta i^{\mathrm{inter}}(Q)$, between intermolecular interference term observed for DL- and L-alanine and between DL- and D-alanine solutions both exhibited a first peak at $Q = 1.6$ Å^{-1}, followed by oscillatory features extending to higher-Q region, implying that there is a difference in the intermolecular structure is present between these solutions. The difference distribution function, $\Delta g^{\mathrm{inter}}(r)$, obtained from the Fourier transform of the $\Delta i^{\mathrm{inter}}(Q)$ between DL- and L-, and between DL- and D-alanine solutions showed an obvious negative peak at $r = 2.8$ Å, which was attributed to the nearest neighbor hydrogen-bonded O···O interaction. The least squares fitting analysis of the observed $\Delta i^{\mathrm{inter}}(Q)$ showed that the intermolecular O···O distance and the difference in the coordination number between DL- and L-, and between DL- and D-alanine solutions are 2.76(2) Å and −0.18(1), and 2.81(3) Å and −0.18(1), respectively. It was concluded that the intermolecular hydrogen-bonded network in aqueous L- and D-alanine solutions is stronger than that in the DL-alanine solution.

The optical activity of amino acid molecules plays an important role in the extended fields of chemical and biological sciences. Although the chemical properties of D- and L-amino acid molecules are identical, the hydrogen-bonded structure is considered to be different between concentrated aqueous solutions involving the racemic DL- and L- (or D-) amino acid molecules. In fact, it is known that L- and DL-amino acid molecules have slightly different solubility in water.[1] This solubility difference is enhanced when heavy water is used as the solvent.[2] The difference in solubility may be related to the different intermolecular hydrogen-bonded network in the crystalline state.[3] This solubility difference causes a difference in the hydrogen-bonded network of the solvent water molecules at higher solute concentrations. In highly concentrated 2.5 mol % aqueous alanine solutions, the mean distance between molecular center of the nearest neighbor alanine molecules has been estimated to be ca. 11 Å, which implies that on the average, 2 or 3 water molecules are present between the nearest neighbor alanine molecules. Hydrogen bonds among the water molecules should be affected by the interaction between polar functional groups of the alanine molecule as well as neighboring water molecules. According to an earlier Monte Carlo simulation study on chiral discrimination between D- and L-alanine molecules, homochirality is slightly favored for short intermolecular distances.[4] However, experimental study on the effect of the different optical activity of solute molecules on the intermolecular hydrogen bonds among solvent molecules has not been reported, except for our recent neutron diffraction work.[5] Our neutron diffraction study on aqueous 2.5 mol % DL- and L-alanine solutions has shown that the intermolecular nearest neighbor O···H and H···H coordination number in the L-alanine solution are ca. 2% larger than those in the DL-alanine solution.[5] On the other hand, it was difficult to obtain structural information on the intermolecular O···O interaction from the neutron diffraction data, because of the relatively small O···O contribution in the observed total neutron interference term. X-ray diffraction is considered to be one of the most suitable experimental methods to obtain information on the intermolecular O···O structure in aqueous solutions.

In the present paper, we describe the results of X-ray diffraction measurements on aqueous 2.5 mol % DL-, L-, and D-alanine solutions in D_2O in order to investigate the difference in the intermolecular O···O partial structure function between aqueous amino acid solutions with different optical activities. In order to confirm the reproducibility and the reliability of the observed difference function, X-ray diffraction measurements were carried out on the same sample solutions by using both a high-energy X-ray diffractometer installed at the SPring-8 synchrotron facility and a laboratory θ–θ type diffractometer.

Experimental

Materials. DL-$CH_3CH(NH_2)COOH$, L-$CH_3CH(NH_2)COOH$, and D-$CH_3CH(NH_2)COOH$ (natural abundance, Nacalai Tesque, guaranteed grade) were dissolved in D_2O (99.9% D, Aldrich Chemical Co., Inc.) to prepare three aqueous 2.5 mol % alanine solutions with the D content of 96.1%, $[x\text{-}CH_3CH(ND_2)\text{-}COOD]_{0.025}(D_2O)_{0.975}$ (x: DL, L, and D), which was adjusted to the value of samples employed in the previous Time-of-Flight neutron diffraction measurements.[5] The sample solution was sealed in a flat plate acrylate resin cell with a thickness of 2.0 mm, which had X-ray transmission windows made of a Kapton® film with a thickness of 25 μm.

High-Energy X-ray Diffraction Measurements. Synchro-

Published on the web December 13, 2007; doi:10.1246/bcsj.80.2329

tron X-ray diffraction measurements in the transmission geometry were carried out at $26 \pm 2\,^{\circ}$C on the horizontal two-axis diffractometer[6] installed at the beamline BL04B2[7] of the SPring-8 synchrotron radiation facility, Hyogo, Japan. An incident X-ray wavelength $\lambda = 0.2009$ Å was employed. Scattered X-rays were collected by a liquid-N_2 cooled Ge solid-state detector over an angular range of $0.3 \leq 2\theta \leq 48.2^{\circ}$, corresponding to the scattering vector magnitude range of $0.16 \leq Q \leq 25.54$ Å^{-1} ($Q = 4\pi \sin\theta/\lambda$). Measurements were carried out in three parts. The angular step interval was chosen to be $\Delta(2\theta) = 0.1^{\circ}$ in the range of $0.3 \leq 2\theta \leq 10^{\circ}$, $\Delta(2\theta) = 0.15^{\circ}$ in the range of $9 \leq 2\theta \leq 20^{\circ}$, and $\Delta(2\theta) = 0.2^{\circ}$ in the range of $19 \leq 2\theta \leq 48.2^{\circ}$, respectively. The total exposure time was 10.5 h for each sample solution. A measurement on an empty cell was made in advance.

Laboratory X-ray Diffraction Measurements. X-ray diffraction measurements were made at $26 \pm 2\,^{\circ}$C in the transmission geometry using a θ–θ X-ray diffractometer (RAD) manufactured by Rigaku Co. Mo Kα radiation ($\lambda = 0.7107$ Å) was employed. The widths of the divergence and scattering slits were set to be $1/2^{\circ}$. The scattering intensities were detected by using a NaI scintillation counter in the angular range of $3 \leq 2\theta \leq 150^{\circ}$, corresponding to $0.46 \leq Q \leq 17.08$ Å^{-1}. The angular step interval was chosen to be $\Delta(2\theta) = 0.2^{\circ}$ with a fixed counting time of 100 s. Measurements were repeated 3 times in order to minimize any long-term instrumental drift and to reduce uncertainties associated with the counting statistics. A measurement of an empty cell was made in advance. Details of the laboratory X-ray diffraction measurement were previously described elsewhere.[8]

Data Reduction. The observed scattering intensities were corrected for background, polarization,[9] absorption,[9] and double scattering.[10] Analytical expression of the coherent scattering factors and incoherent scattering intensities were used from a paper by Hajdu[11] and from the International Tables for Crystallography.[12] The values of the absorption coefficients and anomalous scattering factors used in the correction procedure for BL04B2 data were taken from those tabulated by Sasaki.[13,14] Data normalization procedure was carried out using the least-squares fit by using high-angle method modified by Habenschuss and Spedding.[15]

The observed total interference term, $i(Q)$, is given by[16–18]

$$i(Q) = [I_{eu}(Q) - \langle f^2 \rangle]/\langle f \rangle^2, \tag{1}$$

where

$$\langle f^2 \rangle = \Sigma c_i [\{f_i(Q) + f_i'\}^2 + f_i''^2],$$

and

$$\langle f \rangle^2 = [\Sigma c_i \{f_i(Q) + f_i'\}^2] + (\Sigma c_i f_i'')^2.$$

Here, $I_{eu}(Q)$ is the normalized coherent scattering intensity in electron units. c_i denotes the number of the i-th atom in the stoichiometric unit, $(CH_3CH(ND_2)COOD)_x(D_2O)_{1-x}$. $f_i(Q)$ corresponds to the atomic scattering factor. The real and imaginary parts of the anomalous scattering factor are denoted by f_i' and f_i'', respectively.

The observed interference term, $i(Q)$, can be divided into intra- and intermolecular contributions,

$$i(Q) = i^{intra}(Q) + i^{inter}(Q). \tag{2}$$

The intramolecular interference term can be expressed as

$$i^{intra}(Q) = x i^{intra}(Q) \text{ (for alanine)} + (1 - x) i^{intra}(Q) \text{ (for } D_2O), \tag{3}$$

where

$$i^{intra}(Q) = \sum_{i \neq j} \sum [\{f_i(Q) + f_i'\}\{f_j(Q) + f_j'\} + f_i'' f_j''] \times \exp(-l_{ij}^2 Q^2/2) \sin(Q r_{ij})/(Q r_{ij})/\langle f \rangle^2. \tag{4}$$

Parameters l_{ij} and r_{ij} denote the root-mean-square amplitude and interatomic distance for the i–j pair, respectively. The intramolecular parameters for D_2O molecule determined in the neutron diffraction studies for pure liquid D_2O were used.[19,20] The intramolecular interference term for alanine molecule was evaluated by applying molecular parameters from single crystal X-ray[3] and gas-phase electron diffraction[21] studies. In the present analysis, calculated intramolecular interference term was subtracted from the observed total $i(Q)$ to obtain the intermolecular interference term, $i^{inter}(Q)$:

$$i^{inter}(Q) = i(Q) - i^{intra}(Q). \tag{5}$$

The intermolecular distribution function, $g^{inter}(r)$, is evaluated by the Fourier transform of the $i^{inter}(Q)$,

$$g^{inter}(r) = 1 + (2\pi^2 \rho r)^{-1} \int_0^{Q_{max}} Q i^{inter}(Q) \sin(Qr) \mathrm{d}Q, \tag{6}$$

where ρ is the number density of the stoichiometric unit, $(CH_3CH(ND_2)COOD)_x(D_2O)_{1-x}$. Since oscillational amplitude of $i^{inter}(Q)$ decays much faster than that of $i^{intra}(Q)$ in the high-Q region, because of larger values of intermolecular distances and r.m.s. amplitudes, truncation errors associated with the Fourier transform with finite upper limit of integral are expected to be much less in the intermolecular distribution function, $g^{inter}(r)$.

The intermolecular difference function, $\Delta i^{inter}(Q)$, between sample solutions involving alanine molecules with different optical activities, was evaluated by the following equation:

$$\Delta i^{inter}(Q)(\alpha - \beta) = i^{inter}(Q) \text{ (for } \alpha) - i^{inter}(Q) \text{ (for } \beta). \tag{7}$$

In the present analysis, three kinds of difference functions from DL–L, DL–D, and D–L combinations were determined. The intermolecular difference distribution function, $\Delta g^{inter}(r)$, was determined by the Fourier transform of the $\Delta i^{inter}(Q)$

$$\Delta g^{inter}(r) = (2\pi^2 \rho r)^{-1} \int_0^{Q_{max}} Q \Delta i^{inter}(Q) \sin(Qr) \mathrm{d}Q. \tag{8}$$

The upper limit of the integral, Q_{max}, was chosen to be 20.0 and 17.1 Å^{-1} for the BL04B2 and RAD data, respectively. In evaluating $\Delta g^{inter}(r)$ for the RAD data, the modification function, $\exp(-0.01Q^2)$, was adopted in order to reduce truncation errors arising from statistical uncertainties involved in the observed $\Delta i^{inter}(Q)$ in the high-Q region.

In order to obtain quantitative information from the observed difference function, least-squares fitting analysis was used. In the refinement procedure, the following model function was employed:

$$\Delta i^{model}(Q) = \Sigma(2 - \delta_{ij}) c_i \Delta n_{ij} [\{f_i(Q) + f_i'\}\{f_j(Q) + f_j'\} + f_i'' f_j''] \times \exp(-l_{ij}^2 Q^2/2) \sin(Q r_{ij})/(Q r_{ij})/\langle f \rangle^2, \tag{9}$$

where $\delta_{ij} = 1 (i = j)$ and $\delta_{ij} = 0 (i \neq j)$. Δn_{ij} stands for the difference in the coordination number between sample solutions with different optical activities. Parameters Δn_{ij}, l_{ij}, and r_{ij} were determined by the least squares fit of Eq. 9 to the $\Delta i^{inter}(Q)$ observed form the BL04B2 data sets. The fitting procedure was performed in the range of $0.5 \leq Q \leq 8.0$ Å^{-1} using the SALS program.[22]

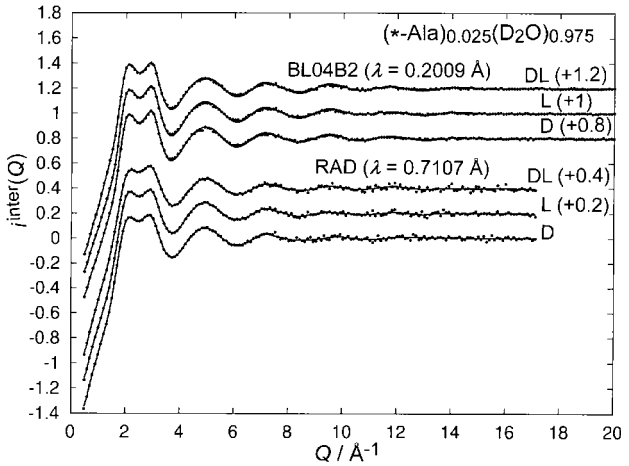

Fig. 1. Intermolecular interference term, $i^{\text{inter}}(Q)$, observed for aqueous 2.5 mol % DL-, L-, and D-alanine solutions in D_2O (dots). Smoothed $i^{\text{inter}}(Q)$ used for the Fourier transform is denoted by a solid line.

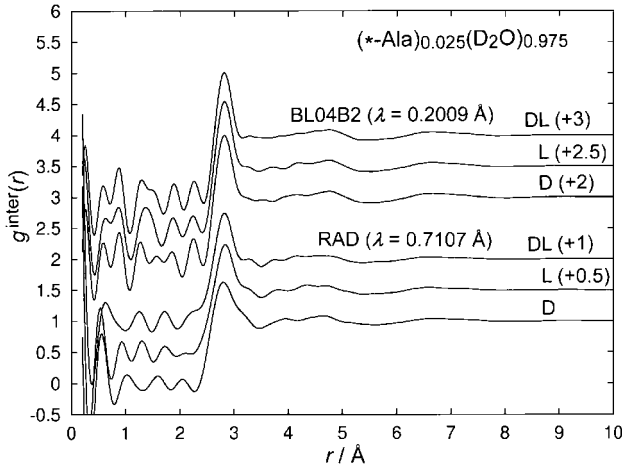

Fig. 2. Intermolecular distribution function, $g^{\text{inter}}(r)$, observed for aqueous 2.5 mol % DL-, L-, and D-alanine solutions in D_2O.

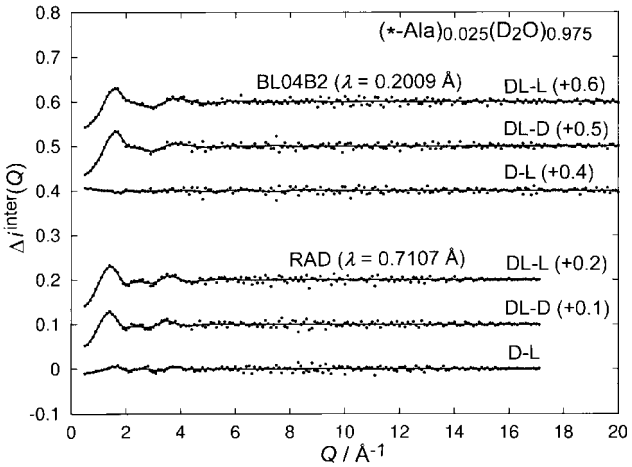

Fig. 3. Intermolecular difference function, $\Delta i^{\text{inter}}(Q)$, between aqueous 2.5 mol % alanine solutions with different optical activities. Smoothed $\Delta i^{\text{inter}}(Q)$ used for the Fourier transform is denoted by a solid line.

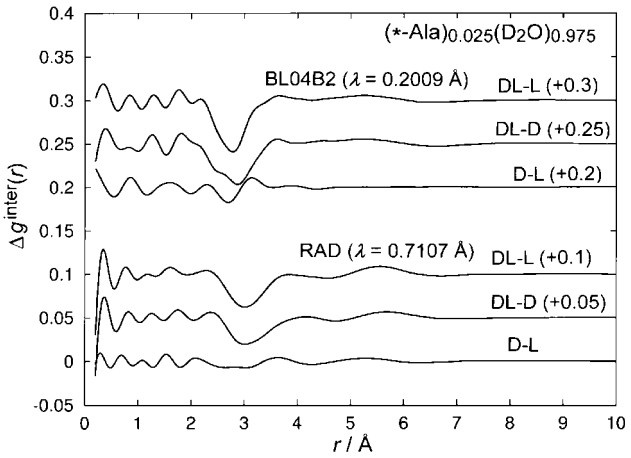

Fig. 4. Intermolecular difference distribution function, $\Delta g^{\text{inter}}(r)$, between aqueous 2.5 mol % alanine solutions with different optical activities.

Results and Discussion

The intermolecular interference term, $i^{\text{inter}}(Q)$, observed for aqueous 2.5 mol % DL-, L-, and D-alanine solutions in D_2O are compared in Fig. 1. The observed $i^{\text{inter}}(Q)$s from BL04B2 and those from RAD agree well with each other except for the interference features in the partially split first diffraction peak at $Q \approx 2\,\text{Å}^{-1}$, which is associated with the difference in the Q-resolution determined by the slit width employed in the scattering measurements. In the present data scale, $i^{\text{inter}}(Q)$s for DL-, L-, and D-alanine solutions look very similar. Intermolecular distribution functions for DL-, L-, and D-alanine solutions are represented in Fig. 2. The dominant first peak at $r \approx 2.8\,\text{Å}$ in the $g^{\text{inter}}(r)$ was mainly attributed to the nearest neighbor hydrogen-bonded O···O interaction. Apparent difference in the height of this first peak between BL04B2 and RAD data sets can be caused from the different values of Q_{max} adopted in the Fourier integral. The overall feature in the $g^{\text{inter}}(r)$ for DL-, L-, and D-alanine solutions again seems very similar to each other.

The difference interference terms derived from the BL04B2 and RAD data sets agree well with each other as shown in Fig. 3. Note that the difference functions from the RAD data are indicated as multiplied by the modification function, $\exp(-0.01Q^2)$. $\Delta i^{\text{inter}}(Q)$ from the DL–L and DL–D combinations were characterized by a first diffraction peak at $Q \approx 1.6\,\text{Å}^{-1}$ and oscillatory features extending to higher-Q region. The results indicate that difference in the intermolecular structure is certainly present between DL- and L-, and between DL- and D-alanine solutions. $\Delta i^{\text{inter}}(Q)$s from DL–L and DL–D combinations agree well within the statistical uncertainties. This implies that the intermolecular structure of D- and L-alanine solution is almost identical as expected. Indeed, the difference function between D- and L-alanine solutions did not exhibit any interference feature within the statistical uncertainties. The difference function $\Delta g^{\text{inter}}(r)$ was obtained by the Fourier transform of the observed $\Delta i^{\text{inter}}(Q)$, as indicated in Fig. 4.

Overall structural features appearing in the $\Delta g^{\text{inter}}(r)$ ob-

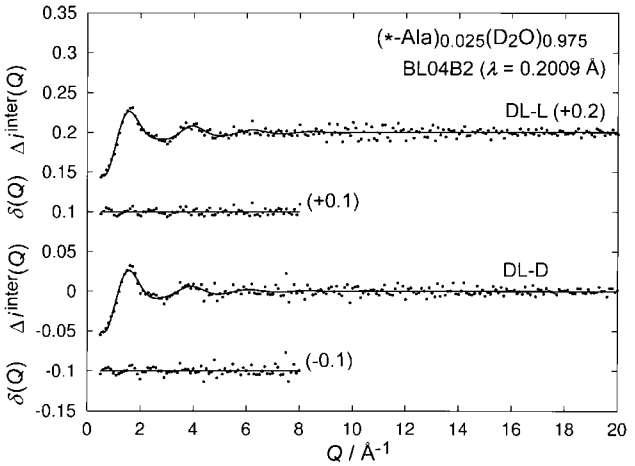

Fig. 5. Observed $\Delta i^{\text{inter}}(Q)$ for aqueous 2.5 mol % alanine solutions in D_2O (dots). The best-fit of the calculated $\Delta i^{\text{model}}(Q)$ is shown by a solid line. Residual function $\delta(Q)$ is indicated below (dots).

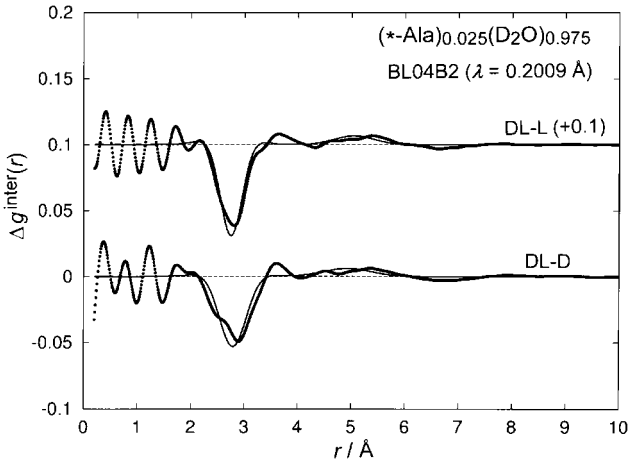

Fig. 6. Observed $\Delta g^{\text{inter}}(r)$ for aqueous 2.5 mol % alanine solutions in D_2O (dots). Fourier transform of the best-fit of the calculated $\Delta i^{\text{model}}(Q)$ is shown by a solid line.

tained from BL04B2 and RAD experiments agree well with each other, which again confirms the differences in the intermolecular structure between DL- and L- and between DL- and D- are undoubtedly present. A dominant negative first peak at $r \approx 3$ Å was observed in $\Delta g^{\text{inter}}(r)$ for the DL–L and DL–D data sets, whereas the $\Delta g^{\text{inter}}(r)$ for the D–L combination did not exhibit any significant structural feature at this distance.

The position of the negative peak in the present $\Delta g^{\text{inter}}(r)$ is very close to the value (2.8 Å) observed for the first intermolecular peak position of the total $g^{\text{inter}}(r)$ shown in Fig. 2. This intermolecular distance is also in good agreement with the nearest neighbor hydrogen-bonded O···O distance (2.84,[23] 2.84,[24] 2.82,[25] and 2.87 Å[26]) determined by X-ray diffraction measurements for pure liquid H_2O. Furthermore, the contribution from the O···O pair is dominated in the present $g^{\text{inter}}(r)$. Thus, we tentatively attributed the negative peak observed in the $\Delta g^{\text{inter}}(r)$ to the nearest neighbor hydrogen-bonded O···O interaction. In order to obtain quantitative information on the difference in the nearest neighbor O···O interaction, least-squares fitting analysis was applied to the difference interference term obtained from DL–L and DL–D data sets observed from the BL04B2 experiment that have better statistical accuracies. In the present fitting procedure, contributions from the first- and second-nearest neighbor O···O interactions were taken into account while evaluating the model function in Eq. 9. The fitting procedure was performed in the range of $0.5 \leq Q \leq 8.0$ Å^{-1} with the SALS program,[22] assuming the statistical uncertainties distribute uniformly. The best-fit results are compared with the observed $\Delta i^{\text{inter}}(Q)$ in Fig. 5. Satisfactory agreement was obtained in the range of $0.5 \leq Q \leq 8.0$ Å^{-1}. The observed and calculated $\Delta g^{\text{inter}}(r)$ curves (Fig. 6) also agree well with each other. The final results of the least-squares fit are summarized in Table 1. The present r_{OO} value is slightly shorter than the nearest neighbor O···O distance observed for pure water.[23–26] The result indicates that small difference in the intermolecular distribution for the hydrogen-bonded O···O interaction might be present between the DL- and L- and DL- and D-alanine solutions. The present value of the position of the second peak is significantly longer than that reported for the second-nearest neighbor O···O distance ($r_{OO} \approx 4.5$ Å) in pure liquid water.[23–26] This suggests that the hydrogen-bonded network is collapsed more significantly in the DL-alanine solution, which is consistent with the present result for the first-nearest neighbor O···O interaction as mentioned above. The difference in the nearest neighbor O···O coordination number, Δn_{OO}, was determined to be −0.18(1) for both the DL–L and DL–D difference functions. The present Δn_{OO} roughly corresponds to ca. 4% of the total O···O coordination number, $n_{OO} \approx 4.4$, which was estimated from the preliminary analysis of the total $i^{\text{inter}}(Q)$ for the DL-alanine solution. The present value of Δn_{OO} is considerably larger than that reported for Δn_{OH} (−0.031(5)) and Δn_{HH} (−0.072(5)), which have been determined from the previous neutron diffraction study.[5] The ratio of the difference in coordination number ($\Delta n_{OO}/n_{OO} \approx 0.04$) is two times larger than the value $\Delta n_{OH}/n_{OH}$ (≈0.019) and $\Delta n_{HH}/n_{HH}$ (≈0.025),[5] which may indicate the characteristics of the intermolecular hydrogen-bonded interaction between water molecules situated between D- and L-alanine, and water molecules situated between L- and L-alanine or between D- and D-alanine molecules. This difference in the hydrogen-bonded structure between DL- and L- and DL- and D-alanine solutions might be due to the difference in the solute–solute interaction in concentrated solutions. If we assume a stronger association of solute molecules with the

Table 1. Results of the Least-Squares Fit of the Intermolecular Difference Interference Terms Observed for Aqueous 2.5 mol % Alanine Solutions in D_2O[a)]

Interactions	Parameters	DL–L	DL–D
The 1st nearest neighbor	r_{ij}/Å	2.76(2)	2.81(3)
	l_{ij}/Å	0.21(3)	0.26(3)
	Δn_{ij}	−0.18(1)	−0.18(1)
The 2nd nearest neighbor	r_{ij}/Å	5.07(8)	4.96(9)
	l_{ij}/Å	0.4(1)	0.5(1)
	Δn_{ij}	0.12(1)	0.12(1)

a) Estimated errors are given in parentheses.

same chirality, as predicted from the MC study,[4] water molecules sandwiched by alanine molecules will be pushed out and hydrogen bonds among water molecules will become more enhanced. In order to examine the difference in the alanine–water interaction between aqueous DL- and L- (or D-) alanine solutions, it is necessary to conduct neutron diffraction measurements for $^{14}N/^{15}N$ isotopically substituted samples.[27] Along this line, neutron diffraction measurements and data analysis are now in progress.

This work was partially supported by Grant-in-Aid for Scientific Research on Priority Area (No. 1641205), Scientific Research (C) (No. 16550049), and Creative Scientific Research (No. 16GS6417), from the Ministry of Education, Culture, Sports, Science and Technology. All calculations were carried out at the Yamagata University Networking and Computing Service Center.

References

1 *Kagaku Binran*, Maruzen Co., Ltd., **1993**, p. II–176.
2 Y. Kameda, M. Yaegashi, **2002**, unpublished data.
3 H. J. Simpson, Jr., R. E. Marsh, *Acta Crystallogr.* **1966**, *20*, 550.
4 D. Andelman, H. Orland, *J. Am. Chem. Soc.* **1993**, *115*, 12322.
5 Y. Kameda, M. Sasaki, M. Yaegashi, Y. Amo, T. Usuki, *Bull. Chem. Soc. Jpn.* **2004**, *77*, 1807.
6 S. Kohara, K. Suzuya, Y. Kashihara, N. Matsumoto, N. Umesaki, I. Sakai, *Nucl. Instrum. Methods Phys. Res., Sect. A* **2001**, *467–468*, 1030.
7 M. Isshiki, Y. Ohishi, S. Goto, K. Takeshita, T. Ishikawa, *Nucl. Instrum. Methods Phys. Res., Sect. A* **2001**, *467–468*, 663.
8 Y. Kameda, R. Takahashi, T. Usuki, O. Uemura, *Bull. Chem. Soc. Jpn.* **1994**, *67*, 956.
9 Y. Waseda, *The Structure of Non-Crystalline Materials*, McGraw-Hill, New York, **1980**.
10 C. W. Dwiggins, Jr., D. A. Park, *Acta Crystallogr., Sect. A* **1971**, *27*, 264.
11 F. Hajdu, *Acta Crystallogr., Sect. A* **1972**, *28*, 250.
12 *International Tables for Crystallography*, Kluwer Academic, London, **1999**, Vol. C.
13 S. Sasaki, *KEK Report 90-16*, National Laboratory for High Energy Physics, Japan, **1990**.
14 S. Sasaki, *KEK Report 88-14*, National Laboratory for High Energy Physics, Japan, **1989**.
15 A. Habenschuss, F. H. Spedding, *J. Chem. Phys.* **1979**, *70*, 2797.
16 H. Ohtaki, N. Fukushima, *J. Solution Chem.* **1992**, *21*, 23.
17 R. Caminiti, G. Licheri, G. Paschina, G. Piccaluga, G. Pinna, *J. Chem. Phys.* **1980**, *72*, 4522.
18 Y. Waseda, *Novel Application of Anomalous (Resonance) X-ray Scattering for Structural Characterization of Disordered Materials*, Springer-Verlag, New York, **1984**, p. 25.
19 J. G. Powles, *Mol. Phys.* **1981**, *42*, 757.
20 Y. Kameda, O. Uemura, *Bull. Chem. Soc. Jpn.* **1992**, *65*, 2021.
21 K. Iijima, B. Beagley, *J. Mol. Struct.* **1991**, *248*, 133.
22 T. Nakagawa, Y. Oyanagi, *Recent Developments in Statistical Inference and Data Analysis*, North Holland, Amsterdam, **1980**, p. 221.
23 A. H. Narten, H. A. Levy, *J. Chem. Phys.* **1971**, *55*, 2263.
24 F. Hajdu, S. Langyel, G. Pálinkás, *J. Appl. Crystallogr.* **1976**, *9*, 134.
25 R. Corban, M. D. Zeidler, *Ber. Bunsen-Ges. Phys. Chem.* **1992**, *96*, 1463.
26 K. Yamanaka, T. Yamaguchi, H. Wakita, *J. Chem. Phys.* **1994**, *101*, 9830.
27 Y. Kameda, K. Sugawara, T. Usuki, O. Uemura, *Bull. Chem. Soc. Jpn.* **2003**, *76*, 935.